Non-Relativistic Radio Jets and Parsec-Scale Absorption in Two Seyfert Galaxies

J.S. Ulvestad[1], J.M. Wrobel[1], A.L. Roy[1,2], A.S. Wilson[3],
H. Falcke[2], & T. Krichbaum[2]

ABSTRACT

The Very Long Baseline Array has been used to image the milliarcsecond-scale 15-GHz radio emission from the Seyfert galaxies Mrk 231 and Mrk 348 at two epochs separated by about 1.7 yr. Both galaxies contain parsec-scale double radio sources, whose components have brightness temperatures of 10^9–10^{11} K, indicating that they are generated by synchrotron emission and probably associated with radio jets. The nuclear components of both galaxies are identified by strong variability between epochs, implying that the double sources are apparently one-sided jets. In Mrk 348, the relative component speed is $0.074 \pm 0.035c$ at a separation of 0.5 pc, while the apparent speed in Mrk 231 is $0.139 \pm 0.052c$ at a separation of 1.1 pc (using $H_0 = 65$ km s^{-1} Mpc^{-1}). The lack of observed counterjets is probably due to free-free absorption by torus gas having ionized densities $n_e > 2 \times 10^5$ cm^{-3} within a parsec of the nuclei. This gas density is consistent with X-ray absorption measurements for both galaxies, and also is similar to that inferred in H_2O megamaser galaxies. Except for radio power, the overall properties of the Seyfert radio sources are similar to compact symmetric objects, whose one-sided jets also could be due to free-free absorption by gas having $n_e \sim 5 \times 10^4$ cm^{-3} on scales of 5–10 pc.

Subject headings: galaxies: active — galaxies: individual (Mrk 231, Mrk 348=NGC 262) — galaxies: jets — galaxies: nuclei — galaxies: Seyfert — radio continuum: galaxies

1. Introduction

Seyfert galaxies have weak and small radio sources relative to radio galaxies and quasars, with typical sizes ≤ 500 pc and typical centimeter-wavelength powers of $\leq 10^{23}$ W Hz^{-1} (Ulvestad & Wilson 1989). These sources are apparently produced by weak jets propagating within ionization

---

[1]National Radio Astronomy Observatory, P.O. Box O, Socorro, NM 87801; julvesta,jwrobel@nrao.edu

[2]Max Planck Institut für Radioastronomie, Auf dem Hügel 69, D-53121 Bonn, Germany; aroy,hfalcke,tkrichbaum,@mpifr-bonn.mpg.de

[3]Department of Astronomy, University of Maryland, College Park, MD 20742; wilson@astro.umd.edu

cones (whose axes are determined by the galaxies' central obscuring disks) and interacting with thermal gas in those cones (Falcke, Wilson, & Simpson 1998). The presence of disks is strongly supported by the detection of nuclear H_2O masers in a number of Seyfert 2 galaxies (Braatz, Wilson, & Henkel 1996), by VLBI imaging of those masers in galaxies such as NGC 4258 (Herrnstein et al. 1997), and by HI absorption seen on parsec scales in weakly active galaxies (Peck & Taylor 1998).

It is of considerable interest to measure the speeds of Seyfert radio jets as close to the nucleus as possible, since such measurements present the possibility of differentiating between "intrinsic" and "environmental" effects in Seyferts. Previous measurements of jet speeds in Seyfert cores are rare. In NGC 4151, upper limits of $0.14c$ and $0.25c$ have been measured on scales of 7 and 36 pc (Ulvestad et al. 1998). In NGC 1068, component positions measured with the Very Large Array and with the Very Long Baseline Array (VLBA) 12.5 yr later imply an upper limit of $\sim 0.5c$ for components ~ 20 pc apart (Ulvestad, Neff, & Wilson 1987; Roy et al. 1998).

The galaxies Mrk 231 (UGC 08058) and Mrk 348 (NGC 262) contain two of the strongest radio sources found in Seyferts, and are prime candidates for the measurement of motions in their cores. Within larger-scale VLBI structures, each galaxy contains a double radio source with a total size of ~ 1 pc or less (Halkides, Ulvestad, & Roy 1997; Ulvestad, Wrobel, & Carilli 1999, hereafter UWC). These central sources have now been imaged at two epochs using the VLBA;[4] this *Letter* reports measurements of the component separation speeds on scales of ≤ 1.1 pc.

2. VLBA Observations & Data Analysis

The 10 telescopes of the VLBA (Napier et al. 1994) have been used to observe Mrk 231 and Mrk 348 at left-circular polarization at two epochs separated by ~ 1.7 yr, between 1996 and 1998. The images at 15 GHz have the best combination of resolution and sensitivity for the compact components, and are the subject of this *Letter*. In all cases, 2-bit sampling was employed for four 8-MHz channels, and the central frequency was 15.365 GHz; on-source integration times ranged from 72 to 156 minutes. The first-epoch observations were affected somewhat by poor weather at several stations.

All data were initially calibrated by using measured gains and system temperatures. Residual delays and rates were removed in AIPS (van Moorsel, Kemball, & Greisen 1996) by fitting to the program galaxies or to phase-referencing sources. (Since the first-epoch observations were not phase-referenced, absolute positions have not been derived.) All data were iteratively imaged and self-calibrated in DIFMAP (Shepherd 1997). Final images, made with uniform weighting, had r.m.s. noises of 0.4–0.5 mJy beam^{-1}, except for the second-epoch image of Mrk 348, where

[4]The VLBA is part of the National Radio Astronomy Observatory, a facility of the National Science Foundation operated under cooperative agreement by Associated Universities, Inc.

dynamic-range limitations caused an effective noise of 1.1 mJy beam^{-1}. Two-component Gaussian models were fitted both in the (u,v) plane and in the image plane, using both DIFMAP and AIPS. Results from the different fitting procedures were generally consistent with each other; we use the image-plane fits here. Flux-density errors (all errors are 1σ) are derived by combining a 5% scale uncertainty in quadrature with the fitting error (which includes noise). Estimated size errors are 20% in each axis, with point sources taken to have upper limits of half the beam size.

Error estimates for relative component positions are generally derived from the image-plane fits; they are consistent with the ranges given by the other methods, and with expectations from the measured noises. For the first-epoch map of Mrk 231, the total range of ± 0.03 mas found by the different procedures is greater than the nominal uncertainty of ± 0.009 mas, so the larger error is used.

3. Results

3.1. Mrk 348

Mrk 348 has a redshift $z = 0.014$ relative to the microwave background (de Vaucouleurs et al. 1991), yielding a scale of 0.31 pc mas^{-1} for $H_0 = 65$ km s^{-1} Mpc^{-1} (used throughout). This galaxy is a type 2 Seyfert with a hidden broad-line region (Miller & Goodrich 1990), implying that its disk/torus is seen nearly edge-on. It also contains a 200-mas (60-pc) triple radio source (Neff & de Bruyn 1983), which coincides with optical [O III] emission imaged by Capetti et al. (1996). Our VLBA images (Figure 1) show a small-scale double source that is well-aligned with the larger scale radio and optical emission; measured component properties are given in Table 1. The relative component separation increased from 1.46 mas (0.46 pc) to 1.58 mas (0.50 pc) in 1.65 yr. Since the stronger component was resolved at the second epoch (see below), its centroid may have shifted. We estimate a 3σ upper limit for the shift that is equal to the component size at the second epoch, giving a total 1σ error of 57 μas for the position of the weaker component relative to a fiducial position in the stronger component. The proper motion is then 0.073 ± 0.035 mas yr^{-1}, corresponding to an apparent speed of $\beta_{\rm app} = 0.074 \pm 0.035$. The epoch of zero separation at the current speed is 1977^{+7}_{-20}, so the secondary could have had its genesis during a strong flux outburst in early 1982 (Neff & de Bruyn 1983). Assuming an optically thin spectrum between 10 MHz and 100 GHz, and equal energies in electrons and protons, the synchrotron lifetime of the secondary component is ~ 50 yr, so no particle acceleration is required since the component ejection.

The total flux density of 122 ± 6 mJy in 1997.10 was slightly smaller than the total of 169 ± 9 mJy measured at 1995.26 (Barvainis & Lonsdale 1998), but Mrk 348 since has undergone a major radio flare. The southern component increased by a factor of 5.5 in 1.65 yr, giving a brightness temperature $T_b > 10^{11}$ K and strongly suggesting that it is the galaxy nucleus. The slight resolution at the second epoch, in a position angle (PA) similar to the component separation, indicates that a new component might have been ejected along the same axis.

3.2. Mrk 231

The redshift of Mrk 231 relative to the microwave background is $z = 0.042$ (de Vaucouleurs et al. 1991), and the corresponding scale is 0.93 pc mas^{-1}. Mrk 231 is a Seyfert 1/starburst galaxy with a heavily obscured nucleus and a total infrared luminosity of $\sim 3 \times 10^{12} L_{\odot}$ (Soifer et al. 1989). It contains a 40-pc north-south radio source (Neff & Ulvestad 1988; UWC) embedded within a starburst several hundred parsecs in extent (Bryant & Scoville 1996; Carilli, Wrobel, & Ulvestad 1998). Our VLBA images (Figure 2) show a double source with a position angle differing by about 65° from the larger scale source, as first reported by UWC. The component separation (see Table 1) increased from 1.08 mas to 1.16 mas in 1.77 yr, for a measured proper motion of 0.046 ± 0.017 mas yr^{-1}, corresponding to $\beta_{\rm app} = 0.139 \pm 0.052$. The epoch of zero separation implied by the measured speed is 1973^{+7}_{-15}. Variability by a factor of 2.5 between epochs implies that the weaker, eastern component is the actual nucleus of the galaxy.

4. Nature of the One-Sided Sources

Parsec-scale radio sources are known in several other Seyfert galaxies, and are typically associated with radio jets. In NGC 1068, the parsec-scale source is identified with the accretion torus (Gallimore, Baum, & O'Dea 1997). However, the brightness temperatures in Mrk 348 and Mrk 231 are too high for thermal emission, and instead suggest association of the radio components with outflowing jets. Strong variability in one component in each galaxy indicates that it is close to the active nucleus, and that the double sources represent one-sided jets rather than straddling the nucleus.

4.1. Relativistic Beaming?

The jet/counterjet ratios are $R > 17$ for Mrk 348 and $R > 45$ for Mrk 231. One-sided structures often are associated with relativistic jets having speed βc that are pointing nearly toward the observer, at an angle θ with respect to the line of sight. In that case, (cf. Pearson & Zensus 1987)

$$\beta_{\rm app} \;=\; \frac{\beta \sin\theta}{1 - \beta\cos\theta} \,. \tag{1}$$

The ratio between the flux densities of approaching and receding components is given by

$$R = \left[(1 + \beta\cos\theta)/(1 - \beta\cos\theta)\right]^{3-\alpha} \,, \tag{2}$$

where the flux density $S(\nu)$ at frequency ν is $S(\nu) = S(\nu_0)(\nu/\nu_0)^{+\alpha}$.

In Mrk 348, if the jet components are optically thin, then $\alpha \approx 0.7$. The observed values of $R > 17$ and $\beta_{\rm app} \approx 0.08$ can be caused by relativistic beaming only if $\beta \approx 0.55$ and $\theta \lesssim 5°$.

However, the Mrk 348 disk/torus is edge-on, and the half-angle of the ionization cone is $\sim$45° (Simpson et al. 1996). If the radio jet were inside the ionization cone, this would imply $\theta > 45°$, inconsistent with relativistic motion near our line of sight. In Mrk 231, the slightly higher observed speed (consistent with Mrk 348 within the errors) and higher upper limit on R translate to $\beta \approx 0.69$ and $\theta \lesssim 8°$, whereas the large-scale disk is $\sim$45° from the line of sight (Bryant & Scoville 1996; Carilli et al. 1998). If the radio axis is perpendicular to that disk, then $\theta \approx 45°$, again inconsistent with explaining the one-sided source due to relativistic motion at a small viewing angle.

We conclude that relativistic boosting is not sufficient to account for the observed one-sided radio sources unless the underlying jet flow is much faster than the proper motions of the components, which might then be quasi-stationary shocks. Such an interpretation has been made for the VLBI jet in Centaurus A, which has $\beta_{\rm app} \sim 0.1$, based on the internal evolution of radio components (Tingay et al. 1998). In Mrk 231 and Mrk 348, no such evidence exists at present, since the structures of the jet components are consistent between the two epochs, and the lifetimes do not require particle re-acceleration in shocks.

4.2. Free-Free Absorption

A likely explanation for the one-sided sources is that the "missing" components are in the receding jet and are free-free absorbed by ionized gas. The free-free optical depth at frequency ν is given by

$$\tau_{\rm ff}(\nu) \;\approx\; 8.2 \times 10^{-2}\; T^{-1.35}\; (\nu/{\rm GHz})^{-2.1}\; E \tag{3}$$

(Osterbrock 1989), where T is the temperature in Kelvin and E is the emission measure in cm^{-6} pc. Optical depths of $\tau_{\rm ff}$(15 GHz) $\gtrsim 4$ are required to account for the jet/counterjet ratio, implying $E \gtrsim 3 \times 10^9$ cm^{-6} pc. For a line of sight distance of 0.1 pc and a temperature $T \sim 8000$ K, the average density of ionized material must be $n_e \gtrsim 2 \times 10^5$ cm^{-3} at 0.5–1.0 pc from the galaxy nuclei, about 100 times higher than that required 15–20 pc from the nucleus of Mrk 231 (UWC). This density is also a factor of 10 higher than is required for the free-free absorption $\sim$ 2 pc from the nucleus of 3C 84 (Levinson, Laor, & Vermeulen 1995). Thus, the current results are consistent with weak active galactic nuclei having disks or tori with $n_e \sim 10^5$ cm^{-3} within a parsec of the nucleus, $n_e \sim 10^4$ cm^{-3} at a few parsecs, and a typical narrow-line region density of $n_e \sim 10^3$ cm^{-3} at 20 pc from the nucleus.

Mrk 348 has an X-ray absorption column density of 10^{23} cm^{-2} (Smith & Done 1996), while that in Mrk 231 is 6×10^{22} cm^{-2} (Nakagawa et al. 1997). For a 0.1-pc path length, these values correspond to average densities of $2 - 3 \times 10^5$ cm^{-3}, remarkably consistent with the values required for counterjet absorption. The densities also are consistent with those found from the spectral turnover of the VLBI core in the H_2O-maser galaxy NGC 2639, assuming that the absorption takes place in a warm, weakly ionized medium (Wilson et al. 1998). Therefore, even though no

H_2O maser emission has been detected in Mrk 231 or Mrk 348 (Braatz, Wilson, & Henkel 1996), the one-sided non-relativistic jets support the presence of a torus whose physical properties are similar to those in the megamaser galaxies. If $\tau_{\rm ff}(15\ {\rm GHz}) \approx 4$, then the ionized medium should become optically thin near 30 GHz, and the counterjets might be detectable in very sensitive VLBI observations at 43 GHz.

4.3. Comparison to Other Parsec-Scale Sources

The low jet speeds in Mrk 231 and Mrk 348 are similar to those measured on parsec scales in weak Fanaroff-Riley-I (Fanaroff and Riley 1974) radio galaxies such as Cen A (Tingay et al. 1998) and 3C 84 (Dhawan, Kellermann, & Romney 1998). The receding jet in 3C 84 is known to be free-free absorbed (e.g., Levinson et al. 1995), and the same may be true of the Cen A counterjet. Since the Seyfert jets are non-relativistic when they emerge from the broad-line region, their initial speeds can be highly relativistic only if they are slowed by interactions with the gas in that region. Physics directly related to the central black holes, such as low spin rates (e.g., Rees et al. 1982; Wilson & Colbert 1995), is another promising explanation for the slow speeds of the Seyfert jets.

Both Mrk 348 and Mrk 231, as well as NGC 2639 (Wilson et al. 1998), have spectra that peak at frequencies of 10–20 GHz. The spectral turnovers are consistent with either synchrotron self-absorption or free-free absorption in their cores. The evidence presented in this *Letter* strengthens the case for free-free absorption in the component at the nucleus, since the gas properties required for the spectral turnovers of the cores are similar to the values measured by X-ray absorption and deduced for the obscuration of the counterjets.

The Seyfert radio sources have general characteristics similar to the compact symmetric objects (CSOs), which display gigahertz-peaked spectra, symmetric radio sources on scales of ~ 100 pc, and one-sided jets on scales of 10 pc (Taylor, Readhead, & Pearson 1996). In addition, the outer components of CSOs have speeds of $\sim 0.15c$ (for $H_0 = 65$) relative to their nuclei (Owsianik & Conway 1998; Owsianik, Conway, & Polatidis 1998). The outer VLBI lobes of Mrk 231 and Mrk 348 are ~ 20 pc from their nuclei, corresponding to ages of ~ 700 yr if they have steady advance speeds of $\sim 0.1c$. These ages can be compared to typical ages of $\sim 10^3$–10^4 yr inferred for CSOs (Readhead et al. 1996; Owsianik & Conway 1998; Owsianik et al. 1998). Hence the Seyfert galaxies seem to be somewhat smaller and much less powerful versions of the CSOs.

The relation between Seyfert and CSO jets is of considerable interest. The CSO jets are one-sided at 15 GHz (Taylor, Readhead, & Pearson 1996), and even at 43 GHz (Taylor, private communication), on scales of 10 pc. At least one CSO shows patchy HI absorption with a column density of 2×10^{23} cm^{-2}, on scales of tens of parsecs, and also may show low-frequency free-free absorption of the receding jet (Peck, Taylor, & Conway 1999). If the high-frequency one-sidedness in other CSOs were due to free-free absorption, as we infer for the Seyferts, then $\tau_{\rm ff}(43\ {\rm GHz}) \geq 2$, implying an average ionized density $n_e \geq 5 \times 10^4$ cm^{-3} for a path length of 5 pc; the corresponding column density would be $\sim 8 \times 10^{23}$ cm^{-2}. If free-free absorption is the cause of the one-sidedness in CSOs, this indicates that the tori/disks in the CSOs may be somewhat larger and more dense than in Seyferts. X-ray spectral studies at moderately high energies could be used to search for the absorption due to this gas.

We thank Greg Taylor, Alison Peck, and Jack Gallimore for useful discussions, and Daria Halkides for assistance with the data reduction for the first epoch of Mrk 348. This research has made use of the NASA/IPAC Extragalactic Database (NED) which is operated by the Jet Propulsion Laboratory, California Institute of Technology, under contract with the National Aeronautics and Space Administration.

REFERENCES

Barvainis, R., & Lonsdale, C. 1998, AJ, 115, 885

Braatz, J. A., Wilson, A. S., & Henkel, C. 1996, ApJS, 106, 51

Bryant, P. M., & Scoville, N. Z. 1996, ApJ, 457, 678

Capetti, A., Axon, D. J., Macchetto, F., Sparks, W. B., & Boksenberg, A. 1996, ApJ, 469, 554

Carilli, C. L., Wrobel, J. M., & Ulvestad, J. S. 1998, AJ, 115, 928

de Vaucouleurs, G., de Vaucouleurs, A., Corwin, H. G., Jr., Buta, R. J., Paturel, G., & Fouqué, P. 1991, Third Reference Catalogue of Bright Galaxies (New York: Springer)

Dhawan, V., Kellermann, K. I., & Romney, J. D. 1998, ApJ, 498, L111

Falcke, H., Wilson, A. S., & Simpson, S. 1998, ApJ, 502, 199

Fanaroff, B. L., & Riley, J. M. 1974, MNRAS, 167, 31P

Gallimore, J. F., Baum, S. A., & O'Dea, C. P. 1997, Nature, 388, 852

Halkides, D. J., Ulvestad, J. S., & Roy, A. L. 1997, BAAS, 29, 1375

Herrnstein, J. R., Moran, J. M., Greenhill, L. J., Diamond, P. J., Miyoshi, M., Nakai, N., & Inoue, M. 1997, ApJ, 475, L17

Levinson, A., Laor, A., & Vermeulen, R. C. 1995, ApJ, 448, 589

Miller, J. S., & Goodrich, R. W. 1990, ApJ, 355, 456

Nakagawa, T., Kii, T., Fujimoto, R., Miyazaki, T., Inoue, H., Ogasaka, Y., Arnaud, K., & Kawabe, R. 1997, IAU Symposium 186, Galaxy Interactions at Low and High Redshift, 103

Napier, P. J., Bagri, D. S., Clark, B. G., Rogers, A. E. E., Romney, J. D., Thompson, A. R., & Walker, R. C. 1994, Proc IEEE, 82, 658

Neff, S. G., & de Bruyn, A. G. 1983, A&A, 128, 318

Neff, S. G., & Ulvestad, J. S. 1988, AJ, 96, 841

Osterbrock, D. E. 1989, Astrophysics of Gaseous Nebulae and Active Galactic Nuclei (Mill Valley: University Science Books)

Owsianik, I. & Conway, J. E. 1998, A&A, 337, 690

Owsianik, I., Conway, J. E., & Polatidis, A. G. 1998, A&A, 336, L370

Pearson, T. J., & Zensus, J. A. 1987, Superluminal Radio Sources, eds. J. A. Zensus & T. J. Pearson (Cambridge: Cambridge University Press), 1

Peck, A. B., & Taylor, G. B. 1998, ApJ, 502, L23

Peck, A. B., Taylor, G. B., & Conway, J. E. 1999, ApJ, submitted

Readhead, A. C. S., Taylor, G. B., Xu, W., Pearson, T. J., Wilkinson, P. N., & Polatidis, A. G. 1996, ApJ, 460, 612

Rees, M. J., Begelman, M. C., Blandford, R. D., & Phinney, E. S. 1982, Nature, 295, 17

Roy, A. L., Colbert, E. J. M., Wilson, A. S., & Ulvestad, J. S. 1998, ApJ, 504, 147

Shepherd, M. C. 1997, Astronomical Data Analysis Software and Systems VI, eds. G. Hunt & H. E. Payne (San Francisco: ASP), 77

Simpson, C., Mulchaey, J. S., Wilson, A. S., Ward, M. J., & Alonso-Herrero, A. 1996, ApJ, 457, L19

Smith, D. A., & Done, C. 1996, MNRAS, 280, 355

Soifer, B. T., Boehmer, L., Neugebauer, G., & Sanders, D. B. 1989, AJ, 98, 766

Taylor, G. B., Readhead, A. C. S., & Pearson, T. J. 1996, ApJ, 463, 95

Tingay, S. J., et al. 1998, AJ, 115, 960

Ulvestad, J. S., Neff, S. G., & Wilson, A. S. 1987, AJ, 93, 22

Ulvestad, J. S., Roy, A. L., Colbert, E. J. M., & Wilson, A. S. 1998a, ApJ, 496, 196

Ulvestad, J. S., & Wilson, A. S. 1989, ApJ, 343, 659

Ulvestad, J. S., Wrobel, J. M., & Carilli, C. L. 1999, ApJ, 516, in press (UWC)

van Moorsel, G., Kemball, A., & Greisen, E. 1996, Astronomical Data Analysis Software and Systems V, eds. G. H. Jacoby & J. Barnes (San Francisco: ASP), 37

Wilson, A. S., & Colbert, E. J. M. 1995, ApJ, 438, 62

Wilson, A. S., et al. 1998, ApJ, 505, 587

Table 1. Results of 2-Component Gaussian Fits

No.	Flux Density (mJy)	Size (mas×mas, deg)	T_b[a] (10^9K)	Offset (mas)	PA (deg)
		Mrk 348, 1997.10			
1 (S)	96 ± 5	Unresolved	$> 6.7 \pm 1.9$	0.000	$\cdots$
2 (N)	26 ± 2	Unresolved	$> 1.8 \pm 0.5$	1.460 ± 0.009	-16 ± 1
		Mrk 348, 1998.75			
1 (S)	552 ± 28	0.16×0.11, PA -9 ± 4	238 ± 68	0.000	$\cdots$
2 (N)	17 ± 1	Unresolved	$> 1.8 \pm 0.5$	1.581 ± 0.021	-15 ± 2
		Mrk 231, 1996.94			
1 (E)	17 ± 1	Unresolved	$> 2.2 \pm 0.6$	1.081 ± 0.030	65 ± 1
2 (W)	51 ± 3	0.32×0.18, PA -74 ± 4	6.9 ± 2.0	0.000	$\cdots$
		Mrk 231, 1998.71			
1 (E)	44 ± 3	Unresolved	$> 6.0 \pm 1.7$	1.162 ± 0.004	68 ± 1
2 (W)	60 ± 3	0.30×0.13, PA -88 ± 4	12.0 ± 3.4	0.000	$\cdots$

[a]All brightness temperatures are expressed in the source rest frames, by multiplying the observed brightness temperature by $(1 + z)$.

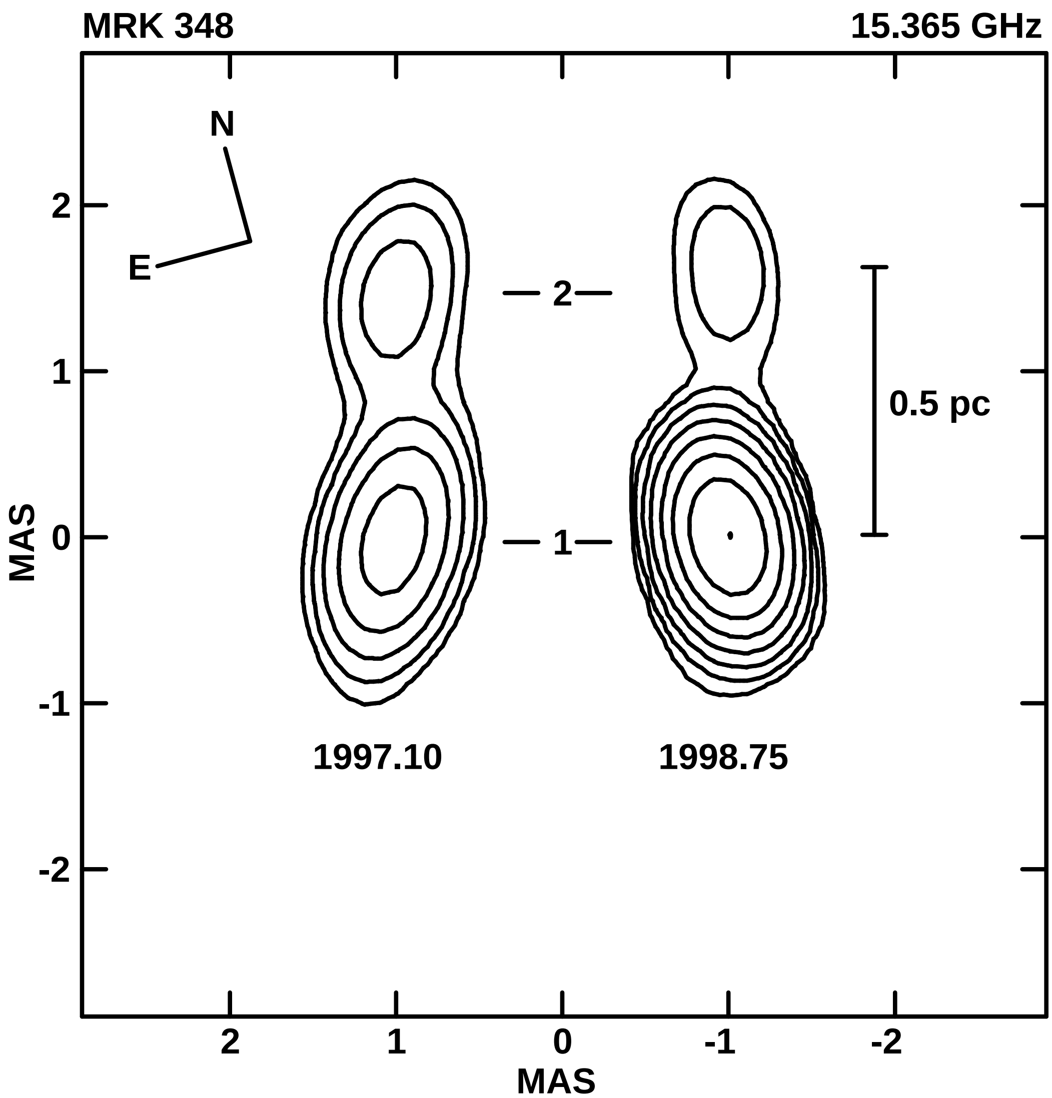

Fig. 1.— 15-GHz VLBA images of Mrk 348 at epochs 1997.10 and 1998.75. The images have been aligned at the southern radio component, rotated by 15°, then offset from each other horizontally. North and East are labeled, as are the two radio components. Both images are contoured logarithmically, with contours starting at 4 mJy beam^{-1} and increasing by factors of 2 to 512 mJy beam^{-1}. The restoring beam at 1997.10 is 0.88×0.49 mas in PA $-30°$, while that at 1998.75 is 0.69×0.42 mas in PA $-2°$.

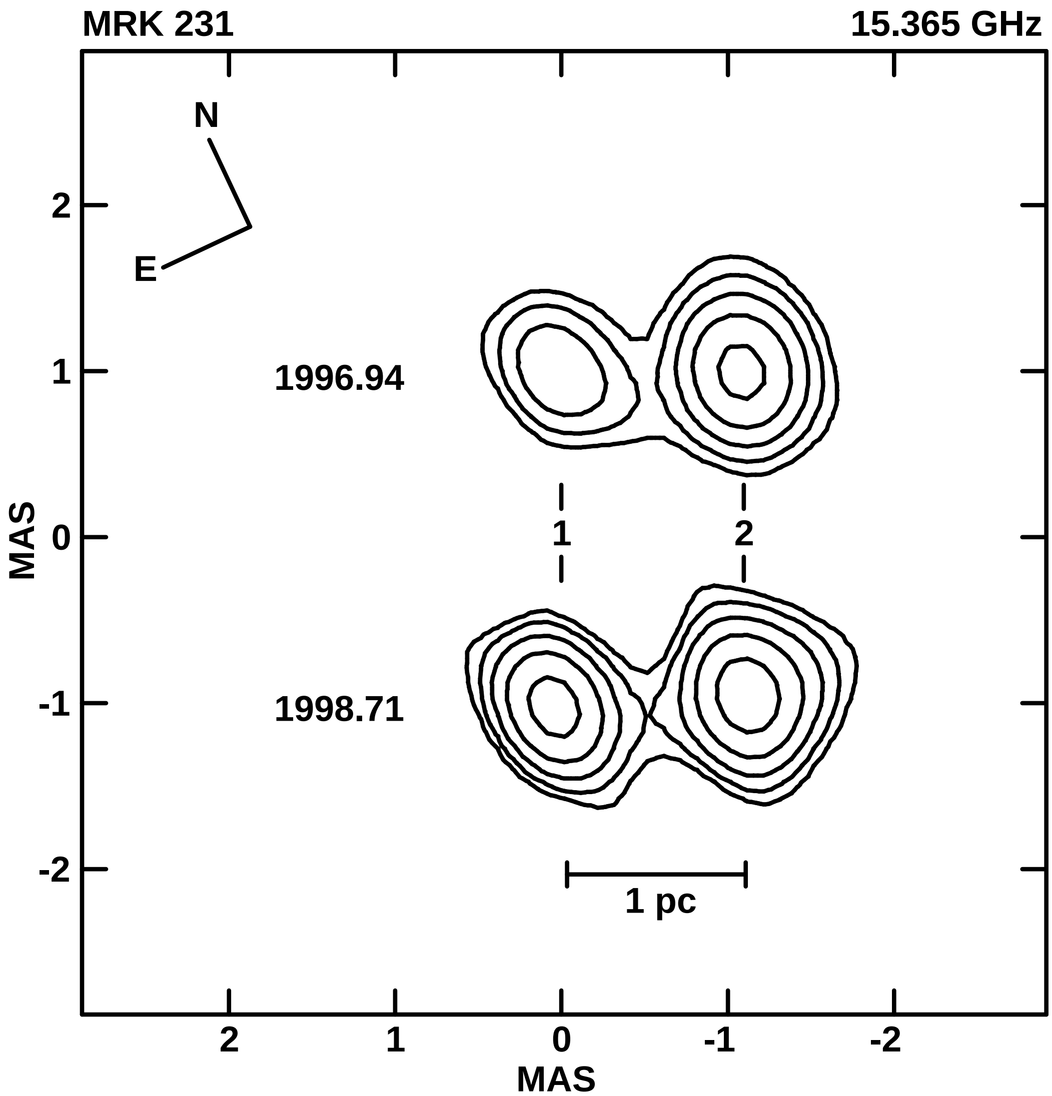

Fig. 2.— 15-GHz VLBA images of Mrk 231 at epochs 1996.94 and 1998.71. The images have been aligned at the eastern radio component, rotated by 25°, then offset from each other vertically. North and East are labeled, as are the two radio components. Both images are contoured logarithmically, with contours starting at 2 mJy beam^{-1} and increasing by factors of 2 to 32 mJy beam^{-1}. The restoring beam at 1996.94 is 0.57×0.42 mas in PA 0°, while that at 1998.71 is 0.54×0.42 mas in PA $-2°$.